A corresponding states equation and compensation effects in crystal growth rates

R. DEARNLEY

British Geological Survey, Murchison House, Edinburgh EH9 3LA

Abstract

Interpretation of grain size measurements in terms of the kinetics of grain growth depends on the ability to define the temperature variation of mineral growth rates. An outline is presented of the application to mineral growth rates of a corresponding states equation (CSE), which provides a relationship of growth rate to a reduced temperature function. Additionally, growth rates exhibit a 'compensation effect' between the pre-exponential constant and the activation energy in the standard Arrhenius equation, analogous to that shown by diffusion data. The general systematics of activation energy, equilibrium temperature and growth rate maxima are controlled by the relationships of the CSE, the standard Arrhenius equation and the compensation effect, and on this basis the temperature variation of growth rate between the equilibrium and the glass temperature may be estimated.

KEYWORDS: mineral growth rates, compensation effect, corresponding states equation.

Introduction

A MAJOR hindrance to the study of the kinetics of the crystallisation processes in igneous rocks is the relative paucity of data on the temperature variation of mineral growth rates. In modelling crystallisation and grain growth in a cooling igneous body, it is impractical to measure the temperature dependence of grain growth rates for each mineral. Even if this were to be done there is no certainty of achieving an environment for the experimental crystallisation which is similar to that of the original rock formation, and in addition, the times required for grain growth would be prohibitively long. It is more convenient to use a limited number of defining parameters to generate trial temperature-dependent growth rate curves.

It is the purpose here to define the major parameters which control the form of the growth rate curves and to attempt to outline the systematics of a wide range of such curves.

Corresponding states equation

A corresponding states equation (Gandica and Magill, 1972; Magill *et al.*, 1973) has been shown to approximate closely to the temperature variation of basaltic mineral growth rates (Dearnley, 1983).

The relationship may be expressed by

$$\log (G/G_{MAX}) = f[T_E - T)/(T_E - T_\infty)] = f\theta \quad (1)$$

where G is the growth rate at temperature T; G_{MAX} is the maximum growth rate and $\log (G/G_{MAX}) = 0$ occurs at $\theta = 0.140$, see Fig. 1 and Table 1, T_E is the equilibrium temperature (°C) and T_∞ is a kinetically limiting value of the glass transition temperature (T_g) at infinite time. Growth can only take place within the temperature range from the equilibrium temperature (T_E) to the transition temperature (T_∞).

The concept of a kinetically limiting T_∞ value may be illustrated (using equation 7) by comparing two growth rate curves with the same equilibrium temperature (T_E), say 1200 °C, but with

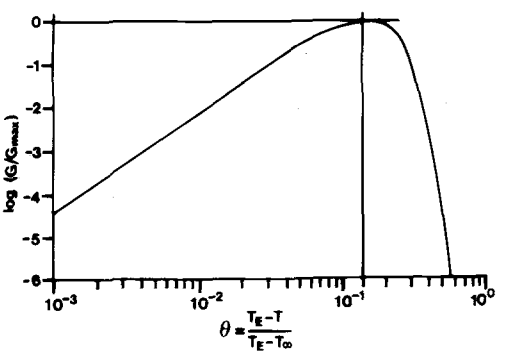

FIG. 1. Standard corresponding states equation (CSE) curve of $\log G/G_{MAX}$ *vs* $\log \theta$. The curve is represented by a 6th degree polynomial, see equation (3).

Table 1 **Corresponding states equation coordinates for the standard growth rate curve**

Reduced temperature function $\theta = (T_E - T) / (T_E - T_\infty)$	Log (G / G_{MAX})
0.02	-1.4086
0.04	-0.7077
0.06	-0.3979
0.08	-0.2152
0.12	-0.0313
0.14	0
0.18	-0.0162
0.24	-0.2951
0.30	-0.9208
0.36	-1.7964
0.43	-3.2041
0.48	-4.3143
0.54	-5.8745
0.60	-7.5687

differing activation energy (for instance of Q = 160 kcals mol^{-1} and Q = 80 kcals mol^{-1}). At decreasing temperatures (for instance during cooling at a given rate) the rate of grain growth falls much more rapidly in the former instance than in the latter. Therefore, in the former case, the growth rate reaches a limiting minimum value more rapidly, and at a higher T_∞ (386 °C) than the corresponding T_∞ (of 42 °C) for the Q = 80 kcals mol^{-1} curve. Such a limiting temperature is similar to that of a closure (or blocking) temperature (see Dodson, 1973, 1976) at which diffusion effectively ceases during cooling.

When the CSE is plotted as a log–log curve (Fig. 1) the power law relations of the high-temperature portion ($\theta \leq 0.04$) are evident, given by

$$G/G_{MAX} = 352.27\ \theta^{2.328} \qquad (2)$$

and, for $\theta \geq 0.43$ the CSE coincides with the Arrhenius expression (equation 4).

For the whole of the curve from $\theta = 0.001$ to 0.60 a sixth degree polynomial (with $r^2 = 0.9998$) closely fits the CSE:

$$\log (G/G_{MAX}) = -21.8640 - 93.6566 \log \theta - 159.2721 (\log \theta)^2 - 138.8832 (\log \theta)^3 - 66.0997 (\log \theta)^4 - 16.1685 (\log \theta)^5 - 1.5841 (\log \theta)^6 \qquad (3)$$

The corresponding states equation (CSE) describes the temperature variation of crystal growth rate of a range of materials and its applications extend beyond the organic molecules for which it was originally devised. It describes equally well the crystallisation of both multiphase and simple congruent melting systems and covers large variations of chemical composition, growth rate (10^{-1} to 10^{-8} cm sec^{-1}), temperature (−40 °C to 1500 °C) and viscosity (10^0 to 10^{13} poise). Such a considerable extension of the CSE to cover materials so diverse as, for instance, glycerol, and blast-furnace slags and natural silicates (Tables 2–4), supports the suggestion (Magill *et al.*, 1973) of a universal relationship.

A preliminary outline of the application of the CSE to the basaltic system (Dearnley, 1983) forms the basis for this present extension, which considers in more detail the relationships involved between the CSE and the standard Arrhenius equation:

$$G = G_O \exp -(Q/RT) \qquad (4)$$

where G_O is the pre-exponential (frequency) factor, Q is the apparent activation energy for growth, R the gas constant and T(°K) is the temperature.

In order to estimate the best fit of the CSE curve to the growth rate *vs* temperature data for a given material, the characteristic value of T_∞ is required and this, in turn, requires the value of Q to be known. Normally, the experimentally measured grain growth rates are presented as a plot of growth rate against temperature, which shows a characteristic peak in growth rate (G_{MAX}) at a certain undercooling (ΔT) from the melting temperature (T_E). The method used to find the best fit to the CSE curve as a whole is based on the individual known values of G and T, together with T_E, an initially estimated (trial) value for Q, and an iterative procedure to obtain T_∞ (as given in Dearnley, 1983). After the value of T_∞ has been found for a given trial Q, the appropriate CSE curve may be determined (based on the parameter θ derived from these values) from equation (3).

The r.m.s.d. (root mean square deviation) is then calculated between the experimental points of the original growth rate curve and the generated trial CSD curve and the whole process is repeated as necessary with another trial value for Q (either incremented or decremented as required) with the object of decreasing the r.m.s.d. to a minimum. At this point the best fit of the experimental data to the CSE curve is obtained and the growth rate curve is completely defined by the determined parameters.

Experimentally determined growth rates at known temperatures for the range of materials in Tables 2–4 are taken from published figures which have a range of scales and units and thus inevitably small errors may occur in the values of

Table 2. **CSE best fits to temperature variation of grain growth data**

No.	T_E °C	T_∞ °C	Q	$LogG_O$	LogG*	$LogG_{MAX}$
LUNAR BASALTS						
1	1180	478	194561	30.08	0.82	-3.66
2	1250	492	194414	29.36	1.47	-2.93
3	1240	345	143770	20.43	-0.33	-4.22
4	1210	275	125000	17.15	-1.26	-4.91
5	1270	230	115012	16.21	-0.08	-3.52
6	1280	208	109841	15.02	-0.43	-3.76
7	1210	161	100000	14.23	0.31	-3.74
8	1185	164	100228	14.86	-0.16	-3.44
9	1270	147	97977	13.75	-0.12	-3.25
10	1310	122	94228	12.05	-0.95	-3.95
11	1360	93	90826	11.95	-0.20	-3.09
12	1365	0	77253	10.06	-0.25	-2.80
13	1340	-32	72777	9.40	-0.46	-2.95
14	1310	-67	67715	8.91	-0.44	-2.82
15	1270	-171	54800	7.37	-0.39	-1.70
ALBITE-ANORTHITE-DIOPSIDE						
16	1255	408	162500	21.11	-2.13	-6.20
17	1390	341	139996	17.22	-1.18	-4.82
18	1391	305	131301	16.24	2.00	-1.52
19	1415	303	131250	16.30	-0.69	-4.20
20	1500	274	125072	16.07	0.66	-2.66
21	1450	275	125000	15.62	-0.23	-3.60
22	1340	277	125000	14.90	-2.03	-5.52
23	1552	168	106735	13.86	1.08	-1.90
GRANITIC MINERALS						
24	670	112	89831	17.72	-3.09	-7.00
25	690	109	88494	16.70	-3.38	-7.22
26	885	115	88210	13.88	-2.76	-6.22
27	850	96	84516	11.95	-4.49	-7.96
28	940	35	73615	9.43	-3.83	-6.89
29	940	-20	64295	8.66	-2.92	-5.70

Lunar basalts : (1) 70019 and (2) 79155 , Klein et al.(1975) ; (3) 14259 , Scherer et al. (1972) ; (4) 67975 , Uhlmann et al. (1977) ; (5) 15498 , Uhlmann and Klein (1976) ; (6) howardite , Hewins and Klein (1978) ; (7) 15286 , Uhlmann and Klein (1976) ; (8) mare basalt , Handwerker et al. (1978) ; (9) 60095 , Uhlmann et al. (1974) ; (10) 14310 , Scherer et al. (1972) ; (11) 65016 , Uhlmann et al. (1974) ; (12) highland basalt , Handwerker et al. (1978) ; (13) 15418 , Uhlmann et al. (1974) ; (14) 15555 , Cukierman et al. (1973) ; (15) Apollo green glass , Uhlmann et al. (1974).

Albite - anorthite , diopside : (16) An10 and (17) An30 , Muncill and Lasaga (1987) ; (18) diopside , Kirkpatrick (1974) and Kirkpatrick et al. (1976) ; (19) An40 , Muncill and Lasaga (1987) ; (20) An75 and (21)An50 , Kirkpatrick et al. (1979) ; (22) An20 , Muncill and Lasaga (1987) ; (23) An100 , Klein and Uhlmann (1974) , Kirkpatrick et al. (1976) .

Granitic minerals : (24) alkali feldspar and (25) quartz from granite ; (26) alkali feldspar and (27) quartz from granodiorite ; (28) and (29) plagioclase from granite and granodiorite , Swanson (1977)

Table 3. **CSE best fits to temperature variation of grain growth data**

No.	T_E°C	T_∞ °C	Q	Log G_O	Log G	Log G_{MAX}
MELILITE						
30	1377	402	157306	21.04	0.21	-3.68
31	1389	354	143750	19.24	0.35	-3.36
32	1395	307	131682	16.60	-0.65	-4.18
33	1417	284	127230	16.47	0.02	-3.44
34	1452	259	122032	15.71	0.26	-3.09
35	1400	256	120543	16.60	0.86	-2.50
36	1420	248	119062	15.50	0.14	-3.18
37	1402	232	115761	15.80	0.70	-2.58
38	1390	169	103748	13.83	0.20	-2.89
39	1487	154	103260	12.65	-0.17	-3.16
40	1470	149	101676	13.41	0.67	-2.30
41	1433	140	99496	12.71	-0.04	-3.00
42	1498	75	90800	10.96	-0.24	-2.95
43	1451	53	86652	10.80	-0.18	-2.86
44	1503	-85	70606	8.09	-0.59	-2.82
LEAD BORATES						
45	696	319	181249	41.46	0.59	-4.42
46	775	313	160846	34.29	0.75	-3.91
47	760	255	135259	29.28	0.67	-3.74
48	750	248	133847	28.59	0.00	-4.46
49	775	73	79090	16.26	-0.23	-3.71

Melilite : (30) 14 , (31) 13 , (32) 15 , (33) 19 , (34) 12 , (35) 23 , (36) 18 , (37) 26 , (38) 24 , (39) 22 , (40) 25 , (41) 17 , (42) 21 , (43) 16 , (44) 20 . glass numbers from Table 3 in Kruchinin and Ivanova (1968) .

Lead borates : (45 - 47) and (49) , $PbO.B_2O_3$ glasses , Eagan et al. (1970) ; (48) $PbO.2B_2O_3$ glass , DeLuca et al. (1969) .

the points used in this study. Values are taken from the experimental points where possible and not from the smoothed growth curves based on these points in the original figures. A set of calculated values of the parameters T_E, T_∞, Q, log G_O, log G^* and log G_{MAX} is listed in Tables 2–4 for 76 published growth rate *vs* temperature curves.†

The CSE best fits of the measured growth rates at various temperatures for the data from Tables 2–4 are shown in Fig. 2. Growth rates in the whole data set have a log r.m.s.d. of 0.399, that is within a factor of 2.51 of the standard CSE curve. This is probably not significantly in excess of the likely errors in the original growth rate measurements together with the errors inherent in reading off the values from the published graphs. Within the various groups of Fig. 2 the mean log r.m.s.d. values of 0.274, 0.306, 0.335, 0.347, 0.375 and 0.879 correspond respectively to the basaltic minerals of Leontyeva (1947, 1949) (Fig. 2.6–9), lunar basalts (Fig. 2.2), lead borates (Fig. 2.5), anorthite-albite and diopside (Fig. 2.1), mellilite (Fig. 2.4) and granitic minerals (Fig. 2.3). This latter group has the largest deviation, which may be due to the difficulties of measurement in this system. In Table 4 numbers, 50, 58 and 65 are based on the smallest numbers of experimental points in their respective groups and are unreliable; all show apparent values for Q which are too large (see equation 20), but are retained for completeness of the Leontyeva (op. cit.) data set. As can be seen from Fig. 2.1, the albite–anorthite, diopside group (Table 2) shows the least scatter about the standard CSE curve over almost five orders of magnitude and is closely followed by the lunar basalts (Table 2) and lead borates (Table 3).

† A listing of the computer programme in BASIC V for the calculation of the best fit CSE curve to grain growth data as outlined here may be obtained from the author.

Table 4. **CSE best fits to temperature variation of growth rate data**

No.	T_E °C	T_∞ °C	Q	$LogG_O$	Log G*	Log G_{MAX}
PLAGIOCLASE						
50	1250	680	300000	42.43	-0.61	-5.66
51	1225	618	262499	38.20	-0.09	-4.97
52	1225	618	262499	38.23	-0.06	-4.94
53	1200	579	243749	35.96	-0.20	-5.01
54	1300	607	242281	33.28	-0.38	-5.05
55	1275	575	229038	31.88	-0.45	-5.05
56	1240	547	220577	31.91	0.06	-4.56
57	1250	459	181250	24.78	-1.22	-5.50
CLINOPYROXENE						
58	1170	716	362499	54.96	0.07	-5.31
59	1250	627	262499	37.54	-0.12	-4.97
60	1200	591	250000	36.64	-0.44	-5.27
61	1240	563	227677	32.49	-0.39	-5.02
62	1275	531	207987	28.89	-0.47	-4.92
63	1250	515	203420	28.26	-0.92	-5.36
64	1200	435	175000	25.28	-0.68	-4.95
OLIVINE						
65	1225	760	381249	55.28	-0.33	-5.71
66	1250	664	287499	40.75	-0.49	-5.48
67	1275	610	247734	34.44	-0.53	-5.26
68	1240	531	212500	30.44	-0.24	-4.80
69	1225	455	181250	25.37	-1.07	-5.37
MAGNETITE						
70	1200	521	211476	29.13	-2.24	-6.80
71	1250	427	168750	21.67	-2.54	-6.68
72	1330	416	162500	19.80	-2.35	-6.35
73	1330	400	156992	18.98	-2.42	-6.34
74	1300	372	150000	17.92	-2.92	-6.80
75	1300	302	131250	14.83	-3.40	-7.04
76	1300	56	83576	8.55	-3.05	-5.84

Plagioclase : (50) olivine basalt 1 , Leontyeva (1947) ; (51) Caucasian basalt 2 and (53) diabase 101 , Leontyeva (1949) ; (54) basalt glass 221-3 , Leontyeva (1943) ; (55) basalt 34 and (56) basalt glass 221-2 , Leontyeva (1949) ; (57) olivine basalt 17 , Leontyeva (1947) .

Clinpyroxene : (58) Caucasian basalt 2 , Leontyeva (1949) ; (59) olivine basalt 17 , Leontyeva (1947) ; (60) Caucasian basalt 1 , (61) basalt glass 221-2 and (62) basalt 34 , Leontyeva (1949) ; (63) olivine basalt 1 , Leontyeva (1947) ; (64) diabase 101 , Leontyeva (1949) .

Olivine : (65) Caucasian basalt 1 , Leontyeva(1949) ; (66) olivine basalt 17 , Leontyeva (1947) ; (67) basalt 34 , (68) basalt glass 221-2 and (69) Caucasian basalt 2 , Leontyeva (1949) .

Magnetite : (70) diabase 101 , (71) Caucasian basalt 2 , (72) and (73) diabase 101 , and (74) Caucasian basalt 1 , Leontyeva (1949) ; (75) olivine basalt 1 , Leontyeva(1947) ; (76) basalt glass 221-3 , Leontyeva (1943) .

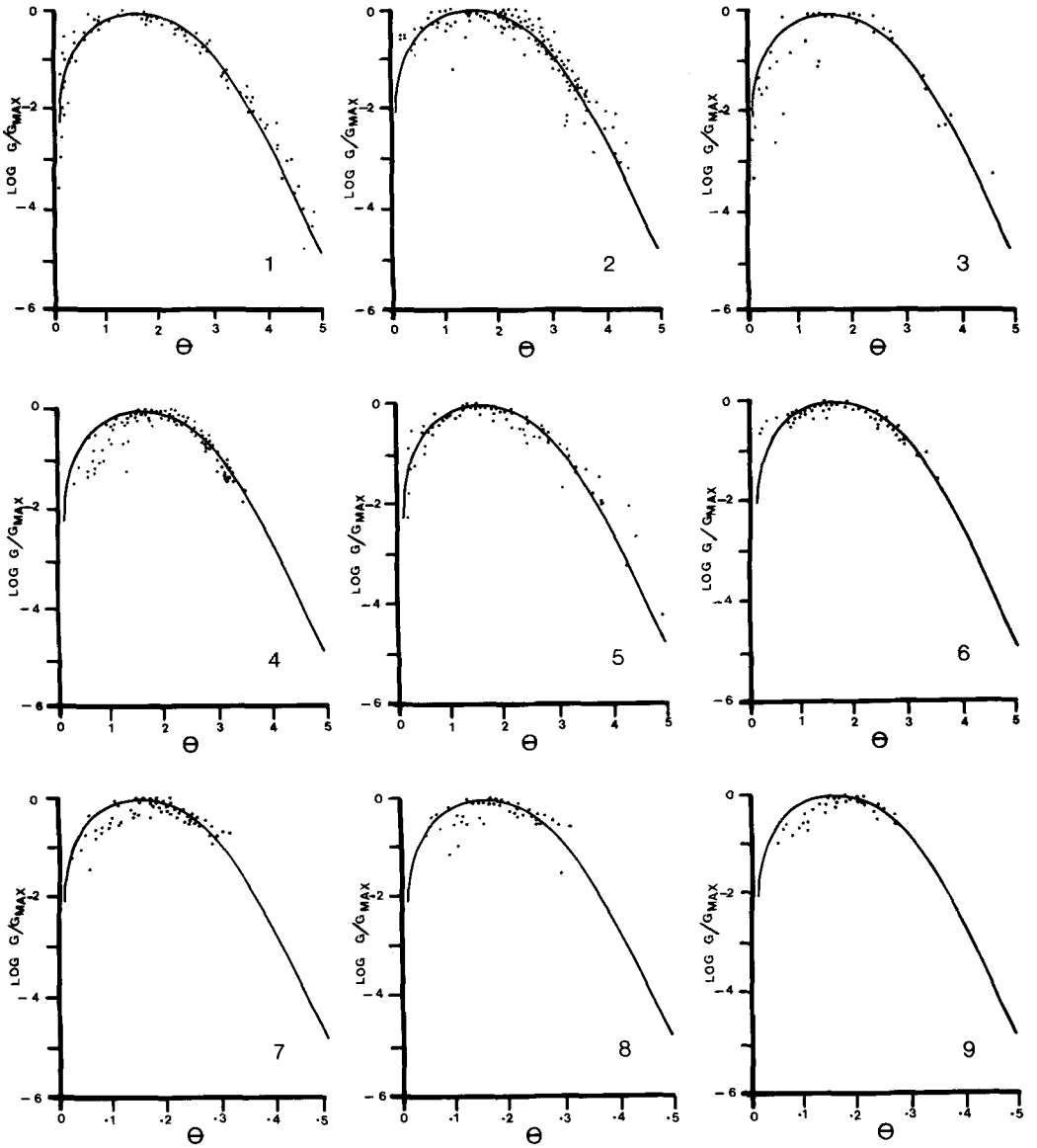

FIG. 2. Growth rate (G) to maximum growth rate (G_{MAX}) ratio plotted against a reduced temperature function, $\theta = (T_E - T)/(T_E - T_\infty)$ for the various mineral groups of Tables 2–4: (2.1) albite–anorthite, diopside; (2.2) lunar basalts; (2.3) granitic minerals; (2.4) mellilite; (2.5) lead borate glasses; (2.6) magnetite; (2.7) plagioclase; (2.8) clinopyroxene; (2.9) olivine. The points plotted correspond to original experimental data points (see references to Tables 2–4) after using a minimum r.m.s.d. procedure to obtain the best fit to the standard CSE curve with the appropriate T_∞ value, see text for details of the method used.

T_∞ and T_g relationships

The parameter T_∞ in equation (1) above may be calculated iteratively from the CSE (Dearnley, 1983), although an alternative explicit expression would be more immediately useful. In deriving such a function the well known 'two-thirds rule' (see, for example Sakka and Mackenzie, 1971) for glass temperature and liquidus temperature, (T_g/T_E) °K $\sim$ 0.66 and the CSE are shown to be directly related.

Using the available glass temperature and

liquidus temperature determinations of 40 lunar basaltic compositions and other basalts (Table 2; Fang *et al.*, 1983, Scarfe, 1977, and Uhlmann *et al.*, 1977) the mean $T_g/T_E = 0.620$, with standard deviation 0.024 and standard error of the mean ±0.004. This is close to the mean $T_g/T_E = 0.627$ for a series of 15 samples, covering the Ab–An range (Arndt and Haberle, 1973, Cranmer and Uhlmann, 1981). For the wider compositional range of (84) inorganic glasses listed in Sakka and Mackenzie (1971) the corresponding values are $T_g/T_E = 0.639$. The combined results (of 139 determinations) yield a mean $T_g/T_E = 0.633$ with a standard error of the mean of ±0.005.

The function θ in equation (1) represents the ratio of the actual growth temperature range ($T_E - T$) to the maximum possible growth temperature range at infinite time ($T_E - T_\infty$). In practice the maximum value of T_∞ approaches T_g and may therefore be estimated from $T_g/T_E = 0.633$. At the other extreme the minimum $T_\infty = -273$ °C.

An exponential function relates the ratio T_∞/T_E to the activation energy, Q for different T_E values as shown in Fig. 3. The linear trends apply between $T_\infty/T_E = 0.633$ and a minimum value of $T_\infty/T_E = 0$, as T_∞ approaches −273 °C. The slope is the same (2.9595) for each T_E and the general relationship is given by

$$Q = a \exp(2.9595\ T_\infty/T_E) \qquad (5)$$

By plotting the constant a (which is the intercept at T_∞/T_E °K = 0, corresponding to $T_\infty = -273$ °C against T °K, a slope of 28.8708 is obtained, with an origin at T °K = 0, and hence

$$Q = 28.8708\ T_E \exp(2.9595\ T_\infty/T_E) \qquad (6)$$

from which

$$T_\infty = 0.3379\ T_E\ (\ln Q - \ln T_E - 3.3628) \qquad (7)$$

This is the desired explicit relationship between T_∞, Q and T_E derived from the CSE, which may be used in (19), below, to provide an expression relating G_{MAX}, T_E and Q, and in (1) to yield

$$\theta = (T_E - T)/[T_E - \{0.3379\ T_E\ (\ln Q - \ln T_E - 3.3628)\}] \qquad (8)$$

or, for use in the polynomial expression in (3). These two equations (19) and (3), using T_∞ from (7) may be used to estimate the temperature variation of growth rate in terms of T_E, Q and G^*.

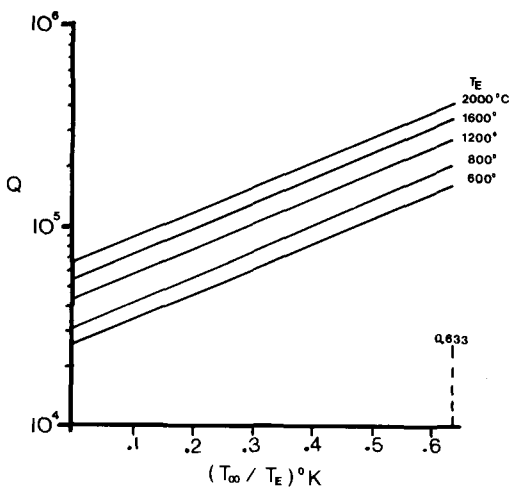

FIG. 3. Relationships of activation energy (Q), at various values of T_E, to the temperature ratio T_∞/T_E. All curves have the same slope (equation 5) and correspond to the general form of equation (6).

Compensation effect

An interesting consequence of the application of the corresponding states equation to the growth rate data of Tables 2–4 is the general correlation which is evident between the hypothetical growth rate limit at infinite temperature (G_O) and the apparent activation energy for growth Q (see Fig. 5) where the relationship takes the form

$$\log G_O = aQ + b \qquad (9)$$

Such a positive linear correlation between log G_O and Q is analogous to that demonstrated by Winchell (1969) and Winchell and Norman (1969) in relation to rates of diffusion in silicates and is termed a 'compensation' effect, see also Hofmann (1980), Lasaga (1981), Hart (1981) and also Shaw (1972) in terms of viscosity estimations. Since the phenomena of diffusion, viscosity and crystal growth are closely related, it is not unexpected that the latter should also be characterised by a well defined compensation effect, although apparently this has not previously been recognised.

For two curves of growth rate plotted against $1/T$, each with the same T_E but with differing G_O and Q values (see Fig. 4*a*), crossover growth rate (G^*) at temperature T^* (= T_E) corresponds to an activation energy (Q) of zero (see Fig. 4*b*).

Since, from (4)

$$\log G^* = \log G_{01} - Q_1/2.303\ RT^* \qquad (10)$$

then, at T^*:

$$(\log G_{01} - \log G_{02})/(Q_1 - Q_2) = 1/2.303RT^*$$

Thus the slope a in Fig. 4*b* is given by

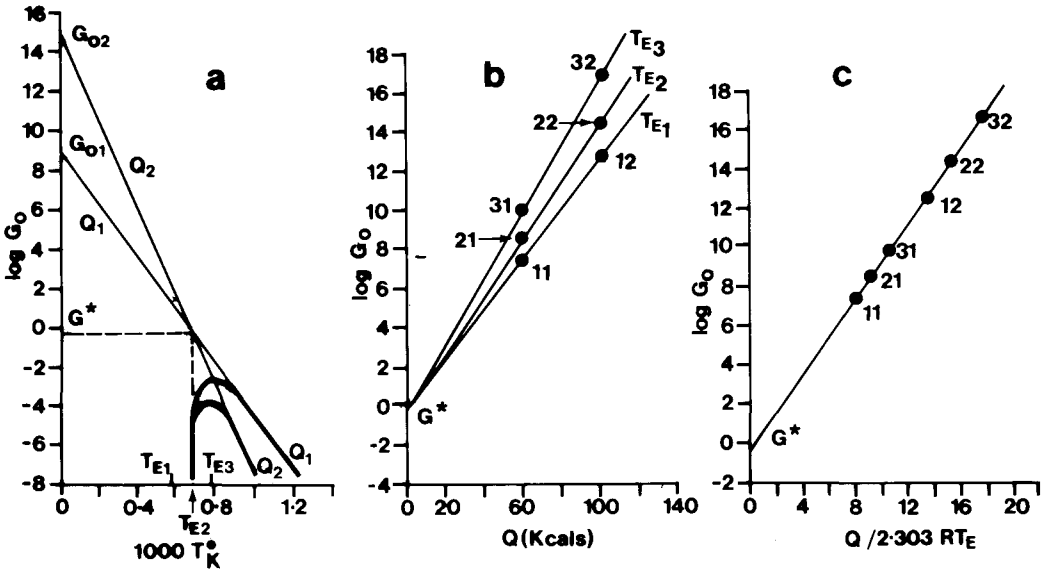

FIG. 4. Growth rate compensation relationships: (*a*) pair of growth rate curves (Q_1 and Q_2), with the same equilibrium temperature (T_{E2}), showing compensation crossover at G^* and T_{E2} and similar pairs may be imagined at T_{E1} and T_{E3} with the same crossover, G^*; (*b*) log G_O *vs* Q (compensation) plot of three pairs of curves as in (*a*), note that the decrease in slope with increasing T_E; (*c*) same data as in (*b*), but with slopes normalised by plotting log G_O against $Q/2.303RT_E$ to yield a single trend.

$$a = 1/2.303RT^* \qquad (11)$$

and from (9)

$$b = \log G_O - aQ \qquad (12)$$

with the crossover temperature at

$$T^* = T_E = 1/2.303\ Ra \qquad (13)$$

and where the crossover growth rate $G^* = 10^b$ (i.e. log $G^* = b$) for any value of T_E.

The final form of the compensation effect equation may be obtained from (9) and (11)

$$\log G_O = Q/2.303RT_E + \log G^* \qquad (14)$$

or alternatively

$$G_O = G^* \exp(Q/RT_E) \qquad (15)$$

and whereas by plotting G_O against Q, as in Fig. 4*b*, the slope is governed by T_E, if G_O is plotted against $Q/2.303RT_E$ then curves for all values of T_E will be superimposed onto a single trend (Fig. 4*c*) with a slope = 1.

The T_E values of the data in Tables 2–4 vary from 670 °C to 1552 °C and, since each point would lie on a different slope, it is not appropriate to plot G_O against Q, as in Fig. 4*b*. Instead the general form (14) is used in Fig. 5 (similar to Fig. 4*c*).

The above discussion is based on the assump-

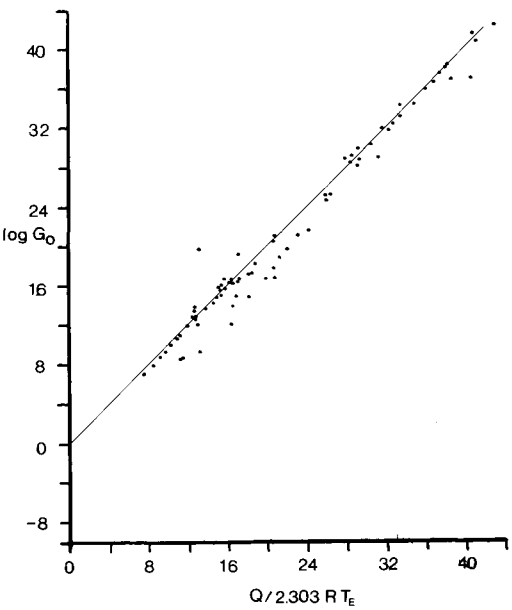

FIG. 5. Compensation plot (as in Fig. 4*c*) for the growth rate data of Tables 2–4. The trend is given by equation (14), setting log $G^* = 0$. Note the scatter involved by not allowing for the variations in G*.

tion of a constant value of the growth rate G^* at a single crossover point at T^* as in Fig. 4. However it is clear from the listings of G^* in Tables 2–4 that this parameter is not a constant and this is apparent also from Fig. 5, which shows a considerable scatter around the trend of G_O against $Q/2.303RT_E$. This is also a feature of the original diffusion compensation law correlation graph of Winchell (1969, Fig. 4), again indicating that G^* is not a general constant, although it may exhibit characteristic values for certain restricted groups of data.

For the data considered here it is apparent that G^* is related to G_{MAX} and increases as G_{MAX} increases (Fig. 6). This is based on 49 mineral growth rate curves from Tables 2–4 including all the data of Table 2 (except the lunar basalts 1 and 2), mellilites from Table 3, and pyroxenes and olivine from Table 4. The remaining minerals, characterised by high Q values, fall on a parallel trend approximately one order of magnitude larger in G^*.

The relationship between G^* and G_{MAX} shown in Fig. 6 may be expressed by

$$G^* = 496\ G_{MAX}{}^{0.8459} \qquad (16)$$

with a correlation coefficient of 0.9533. This regression has relatively large errors and other relationships derived from it (see 28–30, below) are therefore the least reliable and subject to the largest errors.

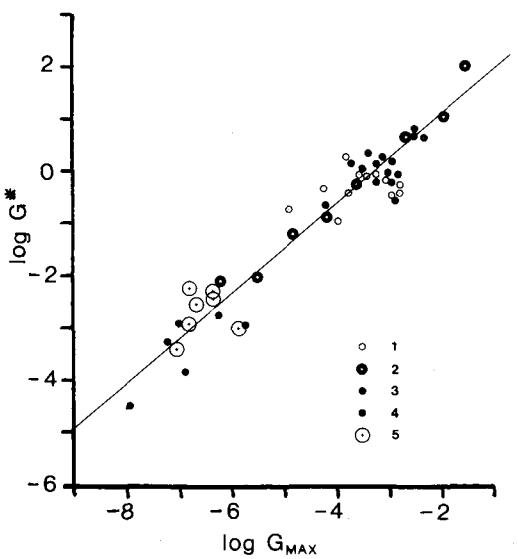

FIG. 6. Relationship of G^* (the crossover growth rate at T_E) to the peak growth rate, G_{MAX}. The regression is given by equation (16). Symbols 1–5 correspond to the groups of minerals listed in Tables 2–4, respectively lunar basalts, albite–anorthite and diopside, granitic minerals and magnetite, see text.

Considering now the connections between the CSE, the Arrhenius and the compensation relationships (equations 1, 4 and 15), we have from (1) an expression for the temperature T_θ at θ given by

$$T_\theta = T_E - \theta(T_E - T_\infty) \qquad (17)$$

When $\theta = 0.14$ (at $\log (G/G_{MAX}) = 0$) the temperature T_θ corresponds to that for G_{MAX}. If however θ is set within the Arrhenius region of the CSE curve (e.g. $\theta = 0.43$) then, from the curve of equation (3): $G_{MAX}/G_\theta = 1/6.25 \times 10^{-4}$ and $G_\theta = 6.25 \times 10^{-4}\ G_{MAX}$. Substituting for T_θ and G_θ in (4) gives

$$G_\theta = 6.25 \times 10^{-4}\ G_{MAX} = G_O \exp[-Q/R\{T_E - \theta(T_E - T_\infty)\}] \qquad (18)$$

Finally, using the compensation relationship (15) to substitute for G_O, an expression for G_{MAX} in terms of T_E, Q, T_∞ and G^* is given by

$$G_{MAX} = 1600\,[G^* \exp(Q/RT_E)] \exp[-Q/R\{T_E - \theta(T_E - T_\infty)\}] \qquad (19)$$

where T_∞ is defined by (7).

Activation energy and growth rate

For a given T_E the maximum and minimum values of Q may be obtained from equation (27) below, by substituting $T_\infty/T_E = 0.633$ and $T_\infty/T_E = 0$ respectively, as shown in Fig. 3, from which

$$Q \text{ max} = 187.95\ T_E°K \qquad (20)$$

$$Q \text{ min} = 28.87\ T_E°K \qquad (21)$$

Similarly, by using (25) below, the value of G^*/G_{MAX} at Q min for any T_E is a constant at 4.46×10^1 cm sec^{-1}, and G^*/G_{MAX} at Q max for any T_E is equal to 1.27×10^5 cm sec^{-1}. These limiting values of G^*/G_{MAX} define the end points of the regression line shown in Fig. 7 when plotted against a normalising factor ($Q/2.303RT_E$) to superimpose the trends for all values of T_E onto a single (power-law) trend joining Q max and Q min, expressed by

$$G^*/G_{MAX} = 1.889 \times 10^{-2}\,[Q/(2.303\ RT_E)]^{4.249} \qquad (22)$$

with a correlation coefficient of 0.995. This simplifies to

$$G^*/G_{MAX} = 2.949 \times 10^{-5}\,(Q/T_E)^{4.249} \qquad (23)$$

and

$$Q = 11.641\ T_E(G^*/G_{MAX})^{0.2353} \qquad (24)$$

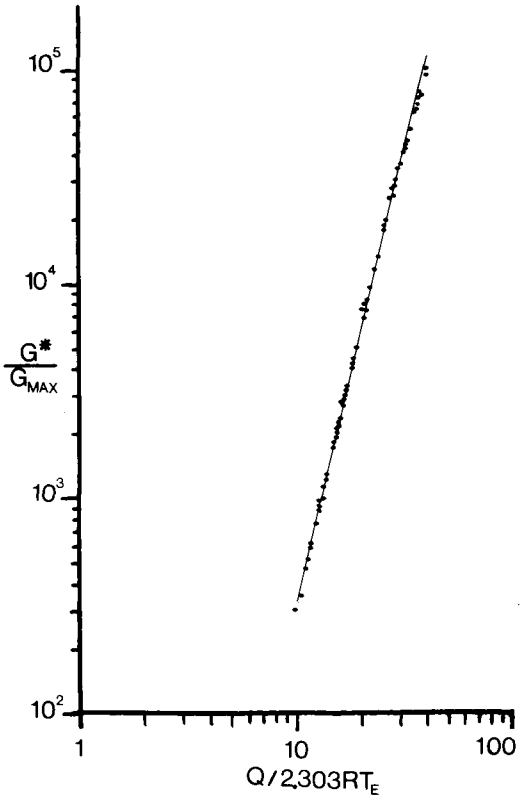

FIG. 7. Relationships of the ratio G^*/G_{MAX} to $Q/2.303RT_E$ for all the minerals of Tables 2–4, for comparison with the compensation plot of Fig. 5. The regression is given by equation (22).

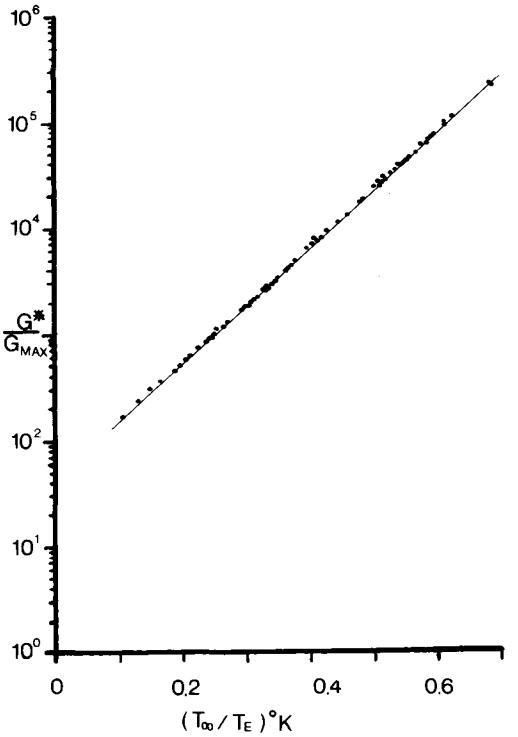

FIG. 8. Plot of the ratio G^*/G_{MAX} against the temperature ratio T_∞/T_E for all the minerals listed in Tables 2–4. The regression is given by equation (25).

For comparison, if this same ratio of G^*/G_{MAX} is plotted against the temperature ratio T_∞/T_E, as shown in Fig. 8, an exponential regression (with correlation coefficient, $r = 0.9993$) is obtained:

$$G^*/G_{MAX} = 44.462 \exp[12.5743\ (T_\infty/T_E)] \quad (25)$$

The influence of these limiting values of G^*/G_{MAX} at Q max and G^*/G_{MAX} at Q min on the overall CSE systematics of growth curves over a range of T_E values may best be appreciated on an Arrhenius diagram (Fig. 9) by using the ratios of G_O/G^* and G^*/G_{MAX} plotted relative to $G^* = 1$. Notable features are the convergence of the Q min slopes at log $G_O/G^* = 6.308$ and the convergence of the Q max slopes at log $G_O/G^* = 41.068$.

At any T_E the value of $G_{O\,MIN}$ represents the pre-exponential factor in equation (4) where $T_\infty = -273\,°C$ and where the activation energy for that T_E is at a maximum. Conversely, $G_{O\,MAX}$ is equal to the pre-exponential factor where $T_\infty/T_E = 0.633$ and the activation energy is at a maximum for that T_E.

In metals, the activation energy for diffusion (Q) approximates to $16RT_E$ °K (McLean, 1965). On this basis, for a typical basaltic composition with an equilibrium temperature of say 1200 °C, the corresponding Q would be 46834 cal. mol^{-1}, which approximates to the Q min value of 42526 cal. mol^{-1} given by equation 21. These two equations have similar constants (respectively, $16R$ and 28.87) but, significantly, the relationship for metals approximates only to the minimum activation energy for silicate minerals. In the latter, Q typically ranges from this lower value up to about 300000 cal. mol^{-1}, see Tables 2–4.

Application of results

The temperature variation of growth rate relationships in Figs. 1 and 2 are defined in terms of the G/G_{MAX} ratios by the CSE, but the absolute G values are determined by G_{MAX} and G^*. Assuming the general applicability of the CSE and within the error limits of G^* as derived from equation (16), then, if T_E and G_{MAX} are

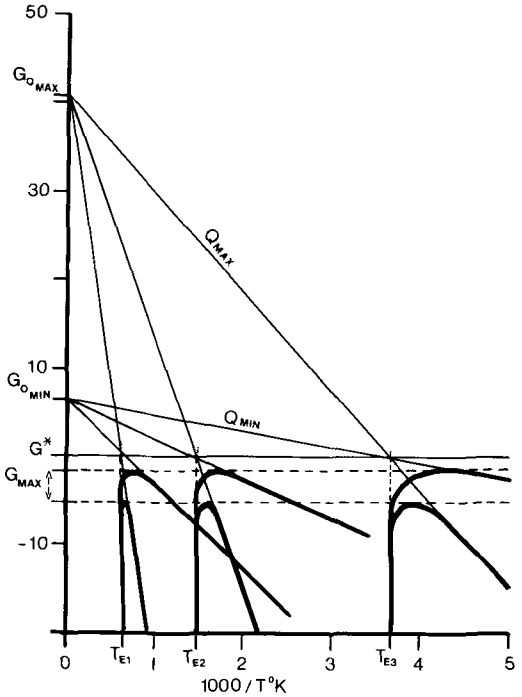

FIG. 9. General relationships of growth rate, activation energy (Q), the pre-exponential factor (log G_O) and equilibrium temperature (T_E), normalised to $G^* = 1$. G^* is the compensation crossover growth rate value at each T_E for the extrapolated Arrhenius trends, $G_{O\,MIN}$ represents the pre-exponential factor for the Q_{MIN} trends at each T_E (equation 21) and $G_{O\,MAX}$ is the corresponding factor for the Q_{MAX} trends at each T_E (equation 20); G_{MAX} defines the range of the growth rate maxima for the range of Q_{MAX} to Q_{MIN} at each T_E.

known, the whole form of the temperature variation of growth rate may be derived.

Relationships derived from the regressions corresponding to Figs. 5–8 may be combined to yield a set of simplifying equations. Combining equations (23) and (25) yields

$$T_\infty/T_E = 0.3379\ (\ln Q - \ln T_E - 3.3628) \quad (26)$$

and also

$$Q/T_E\ 28.8708 \exp[2.9595(T_\infty/T_E)] \quad (27)$$

Combining equations (16) and (22) results in

$$Q = 50.162\ T_E G_{MAX}{}^{-0.0363} \quad (28)$$

and from (27) and (28):

$$T_\infty/T_E = 0.3379 \ln(1.738 G_{MAX}{}^{-0.0363}) \quad (29)$$

Finally, an expression for G_O is obtained from (14), (16) and (28)

$$\log G_O = (10.96\ G_{MAX}{}^{-0.0363}) + (\log 496\ G_{MAX}{}^{0.8459}) \quad (30)$$

The CSE derived relationships outlined above have various practical applications. Firstly, they may be used to extrapolate from incomplete growth rate *vs* temperature determinations. If T_E, Q and G_{MAX} are known, G^* may be obtained from (22–24), then T_∞ from (25–27) and G_O from (14–15). When T_E and Q are known then T_∞ and G^*/G_{MAX} may be found from (26) and (24) respectively. If only T_E and G_{MAX} are known, then the approximate values of the parameters Q, T_∞, G^* and G_O may be derived from equations (28), (29), (16) and (30) respectively, in terms only of these two most commonly available measurements. In this latter case however, using only T_E and G_{MAX}, the errors are greater due to the use of equation (16).

Also, by using measured and/or estimated trial values for T_E, G_{MAX} and Q the kinetics of mineral growth can be modelled over any temperature range of growth as, for instance, in a cooling intrusion.

Although more experimental measurements of crystal growth rate in the major rock forming systems are required to test and complement the above results, these general relationships, based on the best currently available crystal growth data from widely different materials, contribute towards a systematic and practical modelling of crystallisation which does not assume any specific nucleation or transport mechanism for growth.

Acknowledgement

This paper is published by permission of the Director, British Geological Survey (NERC).

References

Arndt, J. and Haberle, F. (1973) Thermal Expansion and Glass Transition Temperatures of Synthetic Glasses of Plagioclase-Like Compositions. *Contrib. Mineral. Petrol.*, **39**, 175–83.

Cranmer, D. and Uhlmann, D. R. (1981) Viscosities in the System Albite-Anorthite. *J. Geophys. Res.*, **86**, 7951–6.

Cukierman, M., Klein, L., Scherer, G., Hooper, R. W., and Uhlmann, D. R. (1973) Viscous flow and crystallisation behaviour of selected lunar compositions. *Geochim. Cosmochim. Acta. Supp.*, **4**, 3, 2685–96.

Dearnley, R. (1983) Basaltic systems and a corresponding states equation for crystal growth rates. *Nature*, **304**, 151–2.

De Luca, J. P., Eagan, R. J., and Bergeron, C. G. (1969) Crystallisation of $PbO.2B_2O_3$ from its supercooled melt. *J. Amer. Ceram. Soc.*, **52**(6), 322–6.

Dodson, M. H. (1973) Closure temperature in cooling geochronological and petrological systems. *Contrib. Mineral. Petrol.*, **40**, 259–74.

——(1976) Kinetic processes and thermal history of slowly cooling solids. *Nature*, **259**, 551–3.
Eagan, R. J., DeLuca, J. P., and Bergeron, C. G. (1970) Crystal Growth in the System PbO-B_2O. *J. Amer. Ceram. Soc.*, **53**(4) 214–9.
Fang, C. Y., Yinnon, H., and Uhlmann, D. R. (1983) Cooling Rates For Glass Containing Lunar Compositions. *J. Geophys. Res.*, **88**, Suppl., A907–A911.
Gandica, A. and Magill, J. H. (1972) A universal relationship for the crystallisation kinetics of polymeric materials. *Polymer*, **13**, 595–6.
Hart, S. R. (1981) Diffusion compensation in natural silicates. *Geochim. Cosmochim. Acta*, **45**, 279–91.
Handwerker, C. A., Onorato, P. I. K., and Uhlmann, D. R. (1978) Viscous flow, crystal growth, and glass formation of highland and mare basalts from Luna 24. *Geochim. Cosmochim. Acta. Supp.*, **9**, 483–93.
Hewins, R. H. and Klein, L. C. (1978) Provenance of metal and melt rock textures in the Malvern howardite. *Proc. 9th Lunar Sci. Conf.*, **10**, 1137–56.
Hofmann, A. W. (1980) Diffusion in natural silicate melts: a critical review. In *Physics of Magmatic Processes* (R. B. Hargraves, ed.), Princeton University Press, New Jersey.
Kirkpatrick, R. J. (1974) Kinetics of crystal growth in the system $CaMgSi_2O_6$–$CaAl_2SiO_6$. *Amer. J. Sci.*, **274**, 215–42.
—— Robinson, G. R., and Hays, J. F. (1976) Kinetics of Crystal Growth From Silicate Melts: Anorthite and Diopside. *J. Geophys. Res.*, **81**, 5715–20.
—— Klein, L., Uhlmann, D. R., and Hays, J. F. (1979) Rates and Processes of Crystal Growth in the System Anorthite-Albite. Ibid., **84**, 3671–6.
Klein, L., and Uhlmann, D. R. (1974) Crystallisation Behaviour of Anorthite. Ibid., **79**, 4869–74.
—— and Uhlmann, D. R. (1976) The kinetics of lunar glass formation, revisited. *Proc. 7th Lunar Sci. Conf.*, 1113–21.
—— Onorato, P. I. K., Uhlmann, D. R., and Hopper, R. W. (1975) Viscous flow, crystallisation behaviour, and thermal histories of lunar breccias 70019 and 79155. *Proc. 6th Lunar Sci. Conf.*, 579–93.
Kruchinin, Yu. D. and Ivanova, L. V. (1968) Crystallisation kinetics of slag glasses. *Izvestiya Akad. Nauk, USSR, Inorganic Materials*, **4**(2), 269–73.
Lasaga, A. C. (1981) The Atomistic Basis of Kinetics: Defects in Minerals. In *Reviews of Mineralogy*, Mineral. Soc., Amer., **8**, 261–300.
Leontyeva, A. A. (1943) Dependence of crystallisation of certain molten rocks (aegirine rocks, basalts and diabases) upon their viscosity. *Trans. All-Russian Mineral Soc.*, **72**(1), 62–9.
——(1947) Crystallisation of two olivine basalts. Ibid., **76**(3), 202–10.
——(1949) The effect of ferric oxide content on the linear rate of crystallisation of solid phases in basaltic glasses. *Trudy. Inst. geol. Nauk, Mosk.*, **106**(3), 33–36.
McLean, D. (1965) The science of metamorphism in metals. In *Controls of Metamorphism* (W. S. Pitcher and G. W. Flinn, eds.), Oliver and Boyd, Edinburgh and London.
Magill, J. H., Li, H. M., and Gandica, A. (1973) Corresponding states equation for crystallisation kinetics. *J. Cryst. Growth*, **19**, 361–4.
Muncill, G. E. and Lasaga, A. C. (1987) Crystal-growth kinetics of plagioclase in igneous systems: One-atmosphere experiments and application of a simplified growth model. *Amer. Mineral.*, **72**, 299–311.
Sakka, S. and Mackenzie, J. D. (1971) Relation between apparent glass transition temperature and liquidus temperature for inorganic glasses. *J. Non Cryst. Sol.*, **6**, 145–62.
Scarfe, C. M. (1977) Viscosity of some basaltic glasses at one atmosphere. *Can. Mineral.*, **15**, 190–4.
Scherer, G., Hopper, R. W., and Uhlmann, D. R. (1972) Crystallisation behaviour and glass formation of selected lunar compositions. *Geochim. Cosmochim. Acta Supp.*, **3**, 3, 2627–37.
Shaw, H. R. (1972) Viscosities of magmatic liquids: an empirical method of prediction. *Amer. J. Sci.*, **272**, 870–93.
Swanson, S. E. (1977) Relation of nucleation and crystal-growth rate to the development of granitic textures. *Amer. Mineral.*, **62**, 966–78.
Uhlmann, D. R. and Klein, L. C. (1976) Crystallisation kinetics, viscous flow, and thermal histories of lunar breccias 15286 and 15498. *Proc. 7th Lunar Sci. Conf.*, 2529–41.
——Klein, L., Kritchevsky, G., and Hopper, R. W. (1974) The formation of lunar glasses. *Geochim. Cosmochim. Acta Supp.*, **5**, 3, 2317–31.
——— and Handwerker, C. A. (1977) Crystallisation kinetics, viscous flow, and thermal history of lunar breccia 67975. *Proc. 8th Lunar Sci. Conf.*, 2067–73.
Winchell, P. (1969) The Compensation Law for Diffusion in Silicates. *High Temp. Sci.*, **1**, 200–15.
—— and Norman, J. H. (1969) A Study of the Diffusion of Radiaoctive Nucleides in Molten Silicates at High Temperatures. In *High Temp. Technol., 3rd Int. Symp., Asilomar, 1967*, 479–92.

[*Revised manuscript received 25 May 1992*]

Explanation of symbols

T_E	Equilibrium temperature
T	Temperature
T_g	Glass temperature
T_∞	Kinetically limiting value of the glass temperature
θ	Temperature difference ratio as in equation 1

Above temperatures in °C or °K as stated in text

G	Growth rate (cm sec^{-1})
G_{MAX}	Maximum growth rate (cm sec^{-1})
G_O	Pre-exponential (frequency) factor in the Arrhenius equation (cm sec^{-1})
G^*	Extrapolated growth rate at compensation 'crossover' point at T_E, see Fig. 4
Q	Activation energy for growth (cal mol^{-1})
R	Gas constant (= 1.986 cal mol^{-1} $°K^{-1}$)